Supporting Information

Yu et al. 10.1073/pnas.1520570112

Lattice Parameters of TAs (T= V, Cr, Mn, and Fe) at Ambient Conditions

The previous investigation of the crystallographic structure of 3d transition metal monoaresenides demonstrated that VAs, CrAs, MnAs, and FeAs are isostructural compounds, which crystallize into the MnP-type structure at ambient conditions (16, 31, 32). We can see from Fig. S1 that the lattice parameter *b* (space group: *Pnma*) of CrAs is larger than those of VAs, MnAs, and FeAs at ambient conditions.

Polymorphisms of CrAs at Various Temperatures and Ambient Pressure

The crystallographic polymorphisms of CrAs at various temperatures and ambient pressure are shown in Fig. S2.

AD-XRD Study on CrAs Carried Out at BI15U1 of SSRF

Fig. S3*A* presents the selected AD-XRD (collected at BL15U1 beamline of SSRF) using the wavelength of 0.6199 Å and a CCD detector) results of CrAs under various pressures. To get further insight into the pressure effect on the structure of CrAs, a slice of the diffraction patterns is magnified in Fig. S3*B*. We can see that the two independent XRD experimental results (X17C, NSLS and BL15U1, SSRF) are consistent. Both of the independent high-pressure AD-XRD experiments were carried out at room temperature.

Documented Pressure-Induced Isostructural Phase Transitions in a Number of Compounds

Xiao et al. (33) performed the AD-XRD study on $PbCrO_3$. The experimental results demonstrated a cubic–cubic isostructural phase transition accompanying a large volume contraction as shown in Fig. S4*A*. The structure of $EuFe_2P_2$ exhibits complex pressure dependence (34). The lattice parameters *a* and *c* show normal decreasing with the pressure increasing up to ∼3 GPa. Then, the lattice parameter *a* shows a downward parabolic trend as the pressure further increases as shown in Fig. S4*B*. The last two cases are about the recently discovered iron-based superconductors. The experimental results suggest that these two iron-based superconductors exhibit pressure-induced isostructural phase transitions, which are indicated by the plateau of the lattice parameters appearing in $Na_{1-x}FeAs$ (35) (Fig. S4*C*) and the bouncing of the lattice parameter *a* in $NdO_{0.88}F_{0.12}FeAs$ (4) (Fig. S4*D*) with the pressure increasing.

Pressure Dependence of the Bonding Lengths of Cr–As (d_{Cr-As})

It can be seen from Fig. S5 that the bonding length correlated to the lattice parameters *a* and *c* shows subtle variation under high pressure, whereas the bonding length correlated to the lattice parameter *b* exhibits contraction as the pressure increases.

Band Scheme of CrAs

The d_{xy} lobes are directed toward the neighboring Cr atoms along the *a* axis, the distance between which is 2.85 Å. A strong covalent bond ought to exist between the indicated Cr atoms, and they form a broad band (O_1). The Cr ions arranged along the *b* axis space so far apart (∼3.45 Å) that their wave functions of the 3*d* electrons have weak overlap, which produces a very narrow band (O_3). The e_g orbitals are directed toward the anion atoms As and form a broad band (O_4 and O_5) due to the strong covalent bond and hybridization with the s and p states. The Fermi level E_F should lie between the valence band and the conduction band, so we have placed it in such a way that it passes through the bands O_2 and O_1^*.

Calculated Band Structure of CrAs

The calculated band structures of CrAs at ambient and 0.4 GPa are shown in Fig. S6. Spin–orbit interaction is evaluated in this calculation by the treatment of noncollinear magnetic structures.

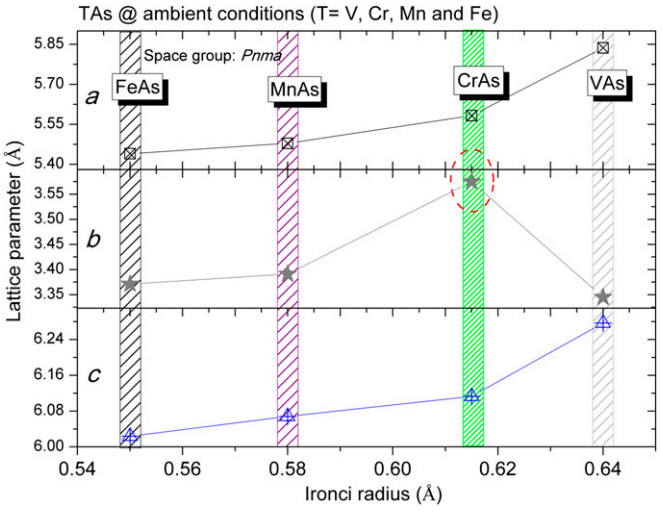

Fig. S1. Lattice parameters of TAs (T = V, Cr, Mn, and Fe) at ambient conditions as a function of the ionic radius.

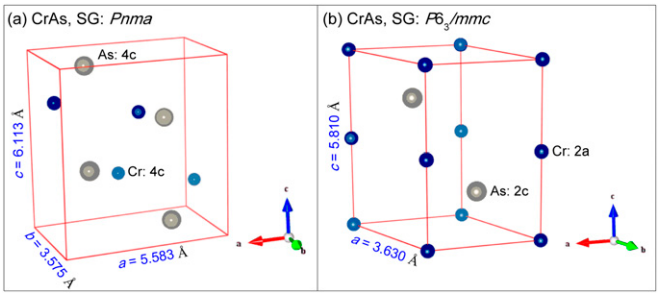

Fig. S2. Crystallographic polymorphisms of CrAs at various temperatures and ambient pressure. (*A*) The orthorhombic structure with space group *Pnma*. (*B*) The hexagonal structure with space group $P6_3/mmc$.

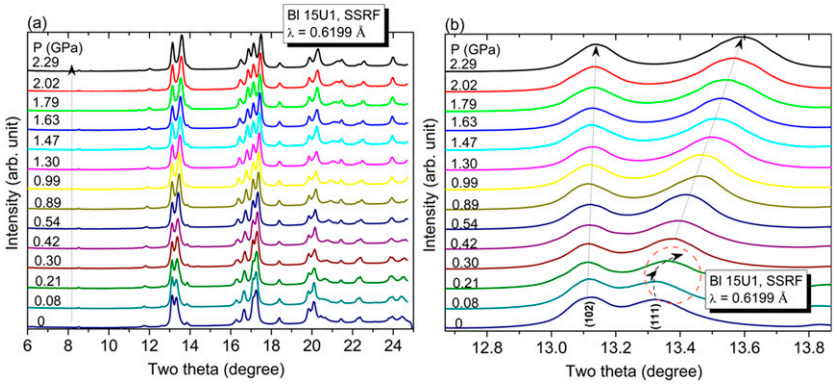

Fig. S3. (*A*) AD-XRD results of CrAs under various pressures. Pressures are indicated in the figure. (*B*) A slice of the diffraction patterns magnified to highlight the pressure dependence. The dotted lines serve as guides to the eyes.

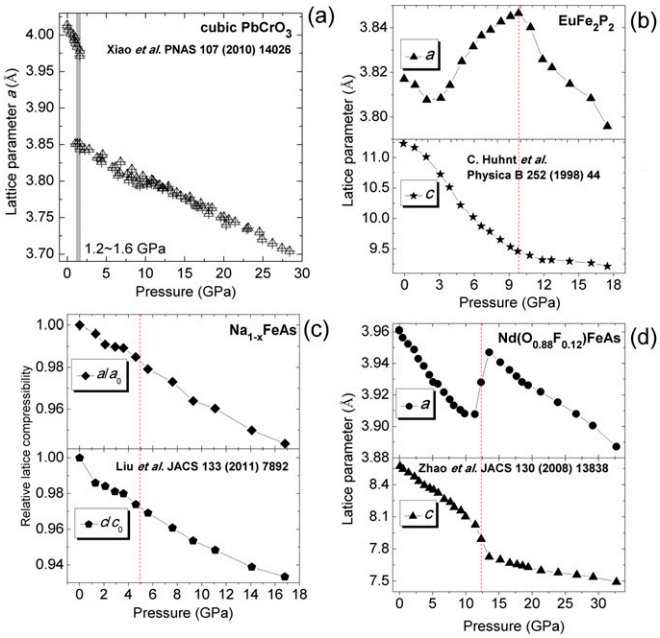

Fig. S4. Pressure-induced isostructural phase transitions in (*A*) $PbCrO_3$, (*B*) $EuFe_2P_2$, (*C*) $Na_{1-x}FeAs$, and (*D*) $Nd(O_{0.88}F_{0.12})FeAs$.

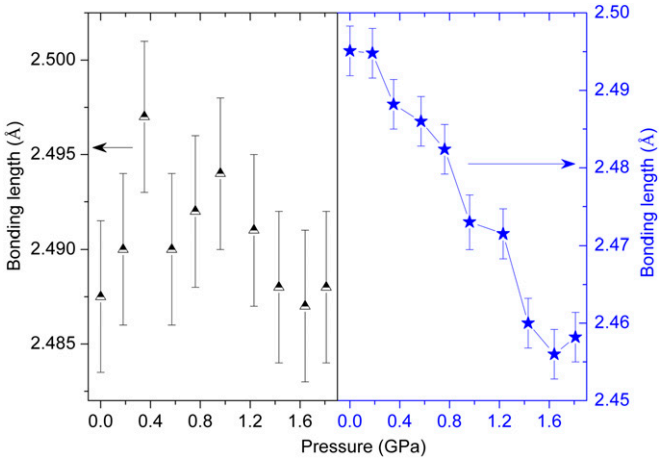

Fig. S5. Pressure dependence of the bonding lengths of Cr–As (d_{Cr-As}).

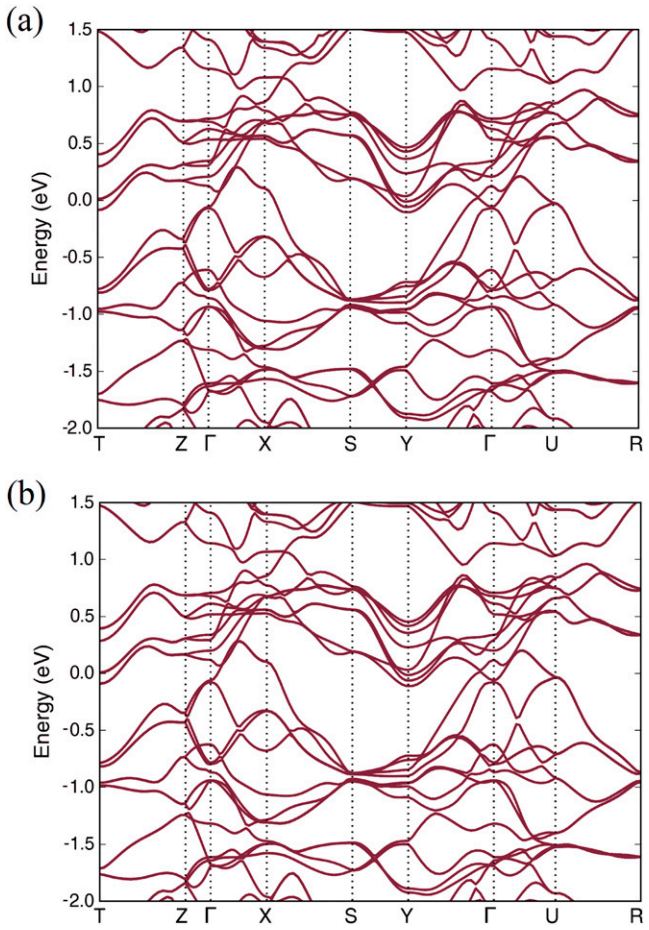

Fig. S6. Calculated band structure of CrAs at (*A*) ambient and (*B*) 0.4-GPa pressures. Spin–orbit interaction is evaluated in this calculation by the treatment of noncollinear magnetic structures.

Table S1. Crystal structure refinement parameters of CrAs

Pressure, GPa	0
Crystal system	Orthorhombic
Space group	*Pnma*
Cell parameters, Å	$a = 5.6584$
	$b = 3.4899$
	$c = 6.2133$
Volume, Å^3	122.696
Wyckoff position	Cr (4c), As (4c)
Atomic parameters	Cr (0.009, 0.25, 0.207)
	As (0.203, 0.25, 0.580)
Agreement factor	$R_p = 1.90\%$, $R_{wp} = 2.66\%$
Pressure, GPa	0.76
Crystal system	Orthorhombic
Space group	*Pnma*
Cell parameters, Å	$a = 5.6587$
	$b = 3.4425$
	$c = 6.2182$
Volume, Å^3	121.13
Wyckoff position	Cr (4c), As (4c)
Atomic parameters	Cr (0.009, 0.25, 0.206)
	As (0.201, 0.25, 0.579)
Agreement factor	$R_p = 3.75\%$, $R_{wp} = 4.64\%$